Iraqi Journal of Physics, 2026
https://doi.org/10.30723/ijp.v24i2.1548

Vol.24, No.2, PP.87-95
P-ISSN: 2070-4003
E-ISSN: 2664-5548

Thickness Dilemma: A Simulation Study of the Performance of PM6:Y6-Based Organic Solar Cells

Duha I. Khalil[1], Dania D. Hameed[2], Hanaa M. Najam[3] and Burak Y. Kadem[2*]
[1]*College of Energy and Environmental Sciences, Al-Karkh University of Science, Baghdad, Iraq*
[2]*College of Science, Al-Karkh University of Science, Baghdad, Iraq*
[3]*College of Science, University of Baghdad, Baghdad, Iraq*
[*]Corresponding author:drburakkadem@gmail.com

Abstract
The effect of active-layer thickness on PM6:Y6 organic solar cells' performance was studied using several characterization techniques, such as current density vs. voltage (J-V), capacitance vs. voltage (C-V), charge vs. voltage (Q-V), charge extraction by linearly increasing voltage (CELIV), and sun-dependent. Results show that increasing thickness increased light absorption and therefore short-circuit current density (J_{SC}), but excessive thickness caused transport limitations and higher recombination, resulting in reduced fill factor (FF). On the other hand, open-circuit voltage (V_{OC}) remained weakly dependent on thickness variation. As a result, power conversion efficiency (PCE) has initially increased and then declined beyond the optimum thickness. C-V and Q-V results indicated reduced charge extraction efficiency and increased series resistance in thick films. Recombination and mobility analyses showed higher loss rates and lower effective mobilities with increasing thickness, consistent with longer transport paths. CELIV confirmed more dispersive, trap-limited transport in thicker layers. Light-intensity-dependent J_{SC} followed a near-linear dependence ($\alpha \approx 1$), and Suns-V_{OC} measurements demonstrated thickness-insensitive voltage governed mainly by recombination kinetics.

Article Info.

Keywords:
PM6:Y6, OSCs, Recombination, Thickness Dependence, Simulated Solar Cells.

Article history:
Received: Jan. 24, 2026
Revised: Feb. 24, 2026
Accepted:Mar. 09, 2026
Published:Jun. 01,2026

1. Introduction

A simulated organic solar cell (OSC) based on the PM6 (PBDB-T-2F):Y6 non-fullerene donor-acceptor system was carried out using the Organic and Hybrid Material Nano Simulation tool (Oghma) [1-3]. BTP-4F (Y6) is a non-fullerene acceptor and an n-type organic semiconductor, while PBDB-T-2F (PM6), a fluorinated derivative within the PBDB-T polymer family, serves as the donor material in polymer solar cells [4] (see Fig.1A). The aim was to investigate the device performance as a function of active-layer thickness. Using suitable interfacial layers is known to enhance the open-circuit voltage (V_{OC}), short-circuit current density (J_{SC}), and fill factor (FF) of organic photovoltaic (OPV) devices, thereby improving their overall efficiency [5]. The simulated device architecture was ITO/ZnO/PM6:Y6/MoOx/Ag (see Fig.1B and C). The active layer thickness was initially optimized at 50nm and then varied up to 300 nm. It is well-known that the active layer thickness is a crucial factor in OSC [6]. Organic semiconductors typically have high exciton binding energies, on the order of several hundred millielectronvolts, much higher than those found in conventional inorganic semiconductors [7]. This is mainly attributed to the low dielectric constant of organic materials. Consequently, free carrier generation is inefficient without donor–acceptor interfaces, often requiring elevated temperatures or strong electric fields to effectively dissociate excitons into free charges [8]. One common way to address this problem is by blending two materials with appropriately offset energy levels in a heterojunction blend [9]. At the heterojunction interface, the energy levels of the donor (D) and acceptor (A) materials are aligned to facilitate easier charge separation and transportation, where electrons and holes can move through their respective material domains. However, a major obstacle to the commercial use of organic solar cells (OSCs) is the very thin active layer, which is usually less than 100 nm thick [10]. Understanding and addressing the factors that restrict active-layer thickness requires establishing a comprehensive energetic framework of photovoltaic

semiconductor junctions. Such an energetic picture is essential for clarifying the roles of different materials and the underlying electronic processes within these devices [11,12]. For such reasons, several characterizations were carried out in this study to investigate the effect of different PM6:Y6 thicknesses using an Organic and Hybrid Material Nano Simulation tool (Oghma). This work aims to provide a deeper understanding of how PM6:Y6 active-layer thickness affects the performance of OSCs, which may inform future optimization of high-efficiency OSCs. The numerical simulation is particularly suitable because it allows thickness to be varied independently of other material properties, provides access to internal physical quantities (band profiles, recombination rates, carrier distributions), and enables systematic exploration of transport and energetic limitations that are difficult to isolate experimentally. Thus, it serves as a powerful complementary tool for understanding thickness-dependent performance trends.

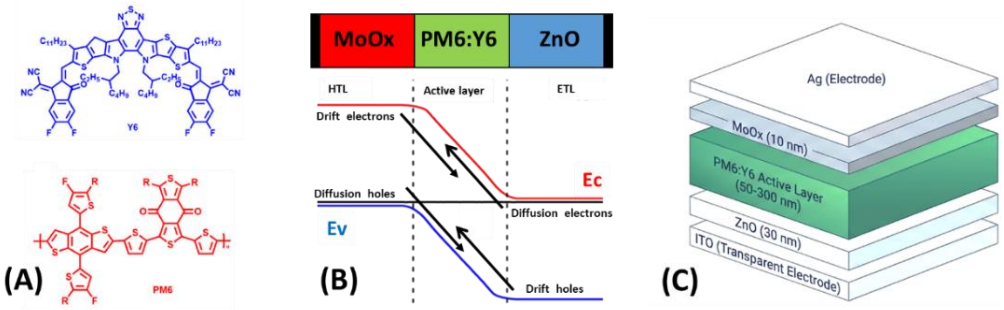

Figure 1: (A) PM6 and Y6 chemical structure, (B) Energy level alignment, and (C) solar cell structure.

The energy levels are assumed to remain fixed during thickness variation. The active-layer thickness is varied as an independent geometrical parameter, while the intrinsic material properties, such as HOMO and LUMO levels (or band edges), work functions of electrodes, and interface energetics, are kept constant. This assumption allows the analysis to isolate the effect of thickness on optical absorption, charge transport, and recombination mechanisms without introducing additional variables related to energetic disorder or morphology changes. Any potential thickness-induced shifts in energy levels, which may arise experimentally due to morphology or interfacial effects, are beyond the scope of the present simulation and are considered as part of future work.

2. Methodology

The solar cell devices with an inverted configuration, shown in Fig. 1C, were simulated using the Organic and Hybrid Material Nano Simulation tool (Oghma). The characteristic parameters of the solar cell layers are illustrated in Table 1. Inverted OSCs are widely used in research because they address several stability and practical fabrication limitations of conventional (regular) OSC architectures. The band alignment between the layers of a solar cell (Fig. 1B) plays a crucial role in determining the overall device performance. Properly aligned energy bands create an internal electric field via band bending, separating photogenerated charge carriers and directing them toward their respective electrodes [13]. To achieve higher efficiency, OSC configuration should be adjusted, and several parameters must be considered, such as carrier diffusion length [10], energy level alignment, enhanced absorption properties, and the use of electron and hole transport layers [14]. In an organic heterojunction, the exciton dissociates based on the diffusion length and the phase separation scale [15]. An effective exciton dissociation arises

at the interface when the exciton diffusion length is higher than the phase separation scale. If not, the recombination process will dominate, leading to energy loss.

In PM6:Y6 organic solar cells, Shockley-Read-Hall (SRH) recombination is a key loss mechanism, with several trap densities (N_t) due to the organic nature. The minority carrier lifetime (τ) is expressed by Eq. (1)[15]:

$$\tau = \frac{1}{\sigma N_t V_{th}} \quad (1)$$

where σ is the capture cross-section of the defect (cm^2), N_t is the trap or defect density (cm^{-3}) and V_{th} is the thermal velocity of charge carriers (cm/s). While the diffusion length (L) is expressed in Eq. (2):

$$L = \sqrt{D\tau} \quad (2)$$

with the diffusion coefficient (D) defined by:

$$D = \mu \frac{kT}{q} \quad (3)$$

where μ is the mobility and kT/q is the thermal energy.

According to these relations, reducing defect density increases the carrier lifetime and extends the diffusion length, thereby suppressing SRH recombination. When the band bending across the PM6:Y6 and transport-layer interfaces is optimal, the resulting internal electric field promotes rapid exciton dissociation, accelerates charge extraction, and minimizes both trap-assisted and interfacial recombination. Consequently, optimal band alignment enhances J_{SC}, V_{OC}, and FF, hence improving overall device performance [16]. For this reason, interface layers were carefully selected.

Table 1: The parameters used in the Oghma software to evaluate the device performance

Parameters	MoOx [11]	PM6:Y6 [5]	ZnO [12]
Thickness (nm)	10	Variable (50-300)	30
Band gap (eV)	3	1.27	3.3
Electron affinity (eV)	2.5	4.03	4
Dielectric permittivity	12.5	6.1	9
CB effective DOS ($1/cm^3$)	2.2×10^{18}	1×10^{19}	1×10^{18}
VB effective DOS ($1/cm^3$)	1.8×10^{19}	1×10^{19}	2×10^{19}
Hole mobility (cm^2/V. sec)	100	2.96×10^{-4}	25
Electron mobility (cm^2/V. sec)	25	1.7×10^{-3}	200
N_D ($1/cm^3$)	0	7.5×10^{16}	1×10^{17}
N_A ($1/cm^3$)	1×10^{18}	0	0

3. Results and Discussions

Fig. 2 shows the differences between thin and thick active layers, where the transport path, recombination rate, electric field, and absorption properties change with the active-layer thickness. Optimizing the latter requires balancing between high photon absorption and reduced charge recombination. Thin layers shorten the travel distance for charge carriers, thereby enhancing transport but restricting the absorption range. On the other hand, thick layers capture more light, yet they may experience lower generation rates due to increased recombination losses [13].

Figure 2: The differences between thin and thick active layers in different perspectives.

Fig. 3A shows the current density-voltage (J-V) curve under illumination for solar cells with different active-layer (PM6:Y6) thicknesses. Fig. 3B shows that the open-circuit voltage (V_{OC}) and short-circuit current density (J_{SC}) vary with different active-layer thicknesses. Results show that V_{OC} shows weak dependence on thickness, while J_{SC} increases steadily and begins to saturate at high active-layer thicknesses, reflecting enhanced light absorption in thicker films. Nevertheless, for the thickest layers, this increase enhances light absorption and exciton generation, but it may result in higher recombination losses and therefore dramatically reduce the FF [16], as shown in Fig. 3C. Beyond a certain thickness, the increase in the active layer thickness has a limited contribution to absorption and is less effective for current. As shown in Fig. 3C, the power conversion efficiency (PCE) initially increases with thickness (primarily driven by increasing J_{SC}), but beyond a threshold, FF loss dominates, leading to a reduction in PCE. This reflects that thick layers harvest more photons but suffer from degraded charge transport and higher recombination. Notably, PM6:Y6 displays an extraordinarily long diffusion length for electrons up to ≈ 300 nm in the acceptor Y6 [10]. Typically, bulk-heterojunction (BHJ) organic solar cells exhibit low charge mobilities and diffusion coefficients, yielding charge-carrier diffusion lengths typically below 20 nm [17]. Although PM6 has a BHJ architecture, it differs from conventional (fullerene-based) BHJs by enabling efficient charge generation at very small energy offsets, reduced recombination losses, and broader absorption due to the non-fullerene acceptor. The highest PCE of 9.1% is found at the device with the optimum thickness of 100nm, associated with a V_{OC} of 0.84 V, J_{SC} of 15 mA.cm^{-2}, and FF of 72%.

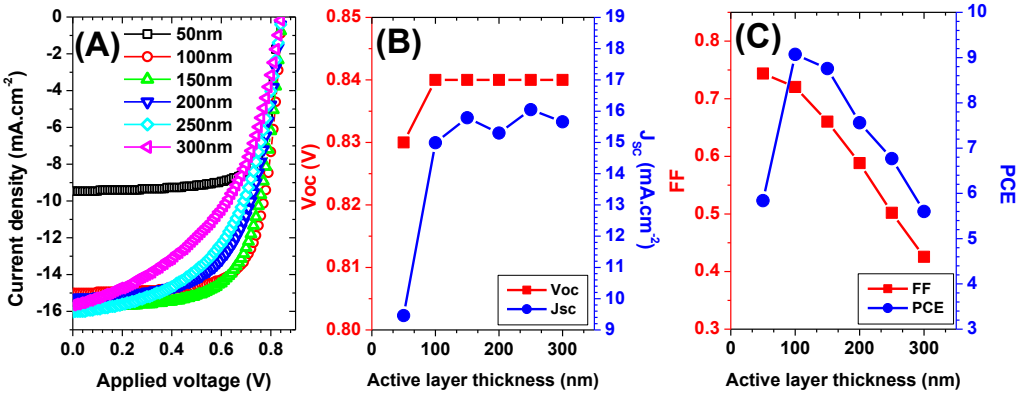

Figure 3: (A) the J-V characteristics, (B) V_{OC} and J_{SC} vs. active layer thickness, and (C) FF and PCE vs. active layer thickness

In BHJ devices, efficient charge extraction relies heavily on electric-field-assisted drift transport, as purely diffusive transport is insufficient for effective collection. Nevertheless, as the active-layer thickness increases, charge transport becomes more challenging: carriers generated deep in the device must travel a longer path to reach the electrodes, increasing the probability of recombination [18]. The consequent drop in FF (and the associated saturation or decline in PCE) is consistent with such transport-limited behavior. Moreover, when the film is too thick, part of

the layer may lie outside the depletion (or space-charge) region, operating more like a "flat-band" region where diffusion (rather than drift) dominates charge transport [10]. In devices with thick active layers, the C-V response becomes noticeably flatter because the voltage-dependent modulation of the depletion region is significantly reduced, as described by Fig. 4A, which shows the Mott-Schottky analysis. When the PM6:Y6 layer is thin, the depletion region can extend through most of the film, leading to a great change in capacitance with applied bias. However, in thick films, only a small portion near the ZnO/PM6:Y6 interface is depleted, while the remaining bulk remains quasi-neutral, resulting in a much weaker dependence of capacitance on voltage. Fig. 4B shows the charge densities versus applied voltage across these solar cells with different active-layer thicknesses. Typically, thicker layers exhibit lower charge densities and higher series resistance, both of which further suppress the voltage sensitivity of the depletion width [19].

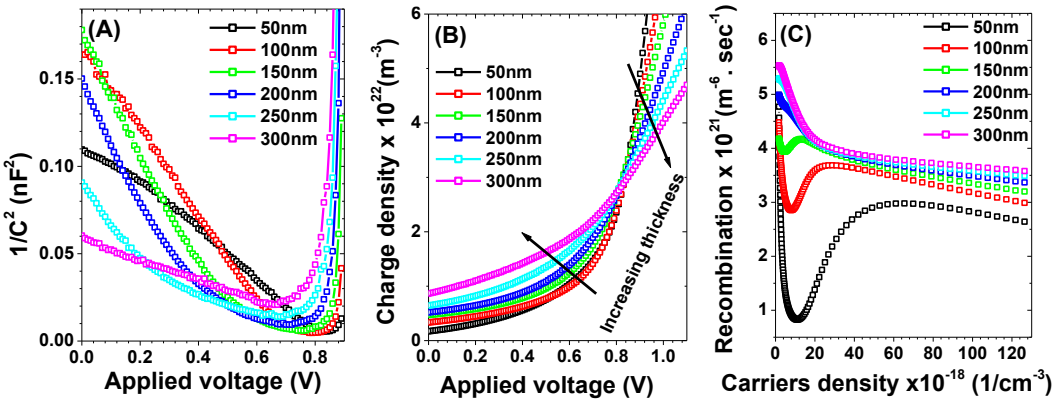

Figure 4: (A) C-V characteristics, (B) Q-V, and (C) recombination rate vs carrier density for the PM6:Y6-based solar cell, at different PM6:Y6 thicknesses.

As mentioned earlier, increasing the active-layer thickness hinders charge extraction and enhances charge recombination because organic materials have short exciton diffusion lengths. This limitation requires careful optimization of the active-layer thickness to balance optical absorption and charge transport. The layer must be thin enough to enable efficient exciton dissociation and rapid carrier mobility [18]. Fig. 4C shows the recombination as a function of charge carrier densities. At a small thickness, when the carrier density is small, the recombination is the lowest. As the thickness increases at the same carrier density, a clear increase in the recombination is observed. As the carrier density increases, all thicknesses show almost the same range of recombination. Generally, OSCs operate through the generation, diffusion, and dissociation of excitons at the donor/acceptor interface, where Charge-Transfer (CT) states form and either separate into free carriers or recombine. In organic semiconductors, excitons naturally have high binding energies because of the low dielectric constant of the organic material. Accordingly, spontaneous thermal dissociation is unlikely, and efficient donor-acceptor interfaces are required to facilitate charge separation [20]. Balanced exciton dissociation combined with rapid charge-carrier transport improves charge mobility and promotes efficient charge extraction, leading to stronger voltage buildup and improved carrier collection at the electrodes. Charge mobility plays a crucial role in determining the efficiency of solar cells. Electron and hole mobilities represent the ability of electrons and holes to move under an applied electric field. In organic semiconductors, charge mobility is strongly affected by factors such as molecular ordering, structural defects, impurities, and temperature [21]. Fig. 5A shows the dependence of charge carrier mobility on the applied voltage. The mobility exhibits field-dependent transport and increases with applied voltage, which is a typical behavior of disordered organic semiconductors. Higher mobilities are required for higher device performance, as they facilitate faster transport of photogenerated carriers across the active layer and reduce recombination losses. Mainly, the charge transport in organic blends is governed by hopping between localized states associated

with conjugated polymer segments [22]. At low electric fields, charge carriers are trapped in the tails of the density of states, limiting drift transport and resulting in lower mobility. Increasing the applied voltage promotes trap filling and field-assisted detrapping, which facilitates hopping transport through higher-mobility percolation pathways, leading to increased mobility and reduced trapping-induced charge losses [23].

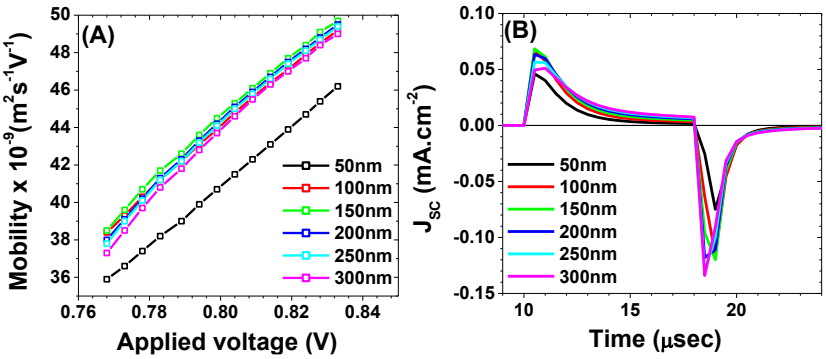

Figure 5: (A) Mobility vs applied voltage and (B) CELIV measurement at different PM6:Y6 thicknesses.

Fig. 5B shows the charge extraction by the linearly increasing voltage (CELIV) technique, which is used to further analyze charge transport in the devices. This method provides details on charge carrier mobility, trapping behavior, and bimolecular recombination processes [24]. For all samples, the CELIV transients show a typical profile: an initial displacement current followed by a negative extraction peak, corresponding to the extraction of mobile charge carriers under a linearly increasing electric field [25]. Both the timing and shape of the extraction peak show a clear dependence on the active-layer thickness. In thick PM6:Y6 layers, the peaks become delayed and broadened, suggesting reduced effective carrier mobility and more dispersive transport influenced by trap states. This effect arises from longer transport pathways and increased energetic disorder in thick films, which limit efficient charge extraction despite improved light absorption.

Fig. 6 shows how charge density (Fig. 6A), carrier mobility (Fig. 6B), V_{OC} (Fig. 6C), and J_{SC} (Fig. 6D) vary with light intensity (SUN) for PM6:Y6 devices of different active-layer thicknesses. For all samples, charge density increased with increasing illumination, demonstrating efficient photocarrier generation. Thick active layers produced high charge densities at the same illumination level due to stronger light absorption and larger active volume. Nevertheless, at higher light intensities, the increase becomes sub-linear, particularly in thicker films, suggesting stronger bimolecular recombination and space-charge effects that restrict efficient carrier extraction [26]. For all thicknesses, mobility increased with increasing light intensity due to trap-filling effects, in which higher carrier densities saturate localized trap states and enable charge transport through higher-mobility pathways [22]. Thin devices show higher mobilities due to shorter transport distances and reduced trapping or scattering [27]. In contrast, thick layers exhibit greater energetic disorder, longer carrier transit distances, and a higher recombination probability, which collectively reduce the effective mobility. Suns-V_{OC} analysis (Fig. 6C) is widely employed to characterize thin-film solar cells, including organic and perovskite photovoltaic devices. It measures V_{OC} as a function of light intensity to probe recombination processes. The slope of the linear region was close to kT/q, and then bimolecular recombination dominated [28]. V_{OC} exhibited only weak sensitivity to active-layer thickness, as the curves for different thicknesses remain closely grouped across the illumination range.

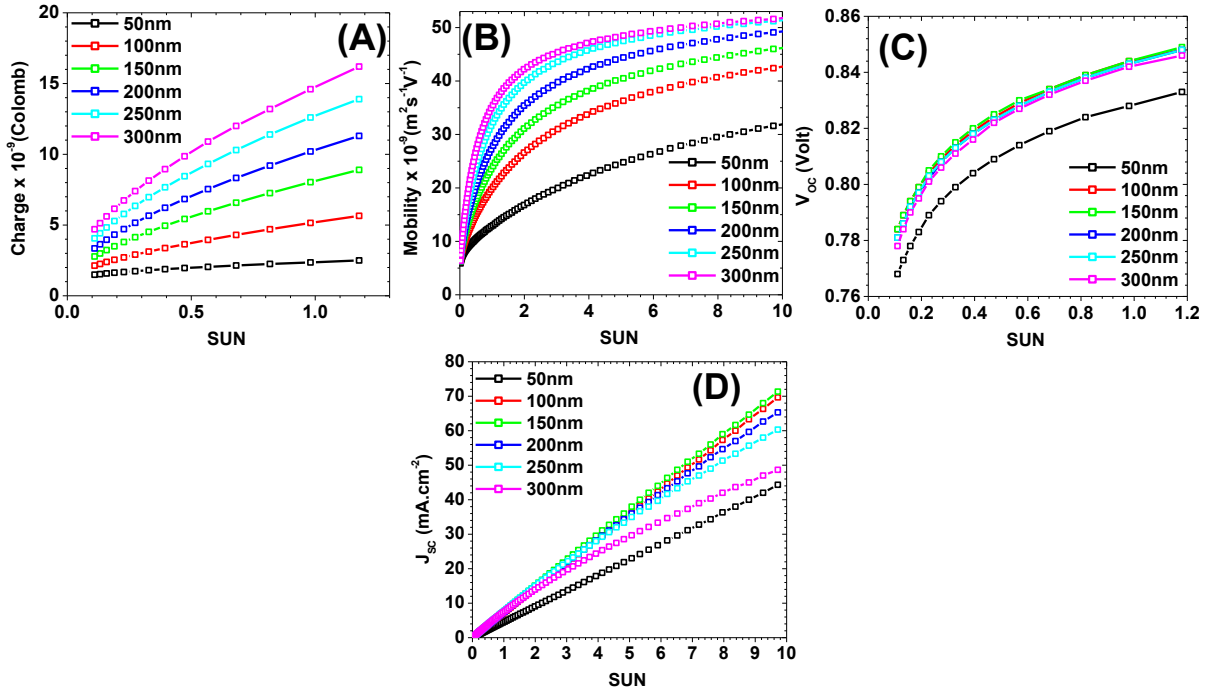

Figure -6 (A) Charge vs SUN, (B) Mobility vs SUN, (C) V_{OC} vs SUN, and (D) J_{SC} vs SUN, for different PM6:Y6 thicknesses

This behavior indicates that V_{OC} is primarily governed by recombination kinetics and energetic alignment rather than by absolute carrier density or transport length. Minor thickness-dependent deviations are likely due to small differences in recombination rates and charge-extraction efficiencies at the donor-acceptor interfaces [26]. The dependence of J_{sc} on the light intensity was further estimated as shown in Fig. 6D. The dominant recombination mechanism at short circuit is independent of the presence of light; J_{sc} follows the power law dependency [29]:

$$J_{SC} = P_{light}^{\alpha} \quad (4)$$

where α is the recombination coefficient, and P is the power of the incident light. The nearly linear behavior observed in Fig. 6D, with $\alpha \approx 1$ for all devices with different PM6:Y6 thicknesses, indicates that charge-carrier losses in the absorber layer are dominated by recombination processes. Carrier losses can arise from interface recombination or bulk recombination. In the bulk, recombination mainly occurs through three mechanisms: Shockley-Read-Hall (trap-assisted), direct band-to-band recombination, and Auger [30].

4. Conclusions

This work demonstrated that active-layer thickness strongly influences the optoelectronic performance of PM6:Y6 organic solar cells. Increasing thickness improved optical absorption and enhanced J_{SC}; however, excessive thickness caused longer carrier transport pathways, higher recombination losses, reduced mobility, and lower charge extraction efficiency, leading to FF and PCE degradation. Electrical analyses confirmed that the thick active layers exhibit transport-limited and trap-assisted recombination behavior accompanied by dispersive charge transport. The optimum device performance was achieved at an active layer thickness of approximately 100nm, where a balance between photon absorption and efficient carrier extraction was obtained. These findings highlight that careful thickness optimization is essential for improving the efficiency and stability of PM6:Y6 based OSC and may provide useful guidance for the design of high-performance organic photovoltaic devices.

Conflict of Interest

The authors declare that they have no conflict of interest.

References

1. B. J. Tremolet de Villers, R. C. MacKenzie, J. J. Jasieniak, N. D. Treat, and M. L. Chabinyc, Linking Vertical Bulk-Heterojunction Composition and Transient Photocurrent Dynamics in Organic Solar Cells with Solution-Processed MoO_x Contact Layers, *Adv. Energy Mater.* **4**(5), 1301290 (2014). https://doi.org/10.1002/aenm.201301290.
2. R. C. MacKenzie, A. Göritz, S. Greedy, E. von Hauff, and J. Nelson, Theory of Stark spectroscopy transients from thin film organic semiconducting devices, *Phys. Rev. B* **89**(19), 195307 (2014). https://doi.org/10.1103/PhysRevB.89.195307.
3. R. Singh, E. Aluicio-Sarduy, Z. Kan, T. Ye, R. C. I. MacKenzie, and P. E. Keivanidis, Fullerene-Free Organic Solar Cells with an Efficiency of 3.7% Based on a Low-Cost Geometrically Planar Perylene Diimide Monomer, *J. Mater. Chem. A.* **2**(35), 14348 (2014). https://doi.org/10.1039/C4TA02851A.
4. M. S. Salem, A. Shaker, and M. M. Salah, Device Modeling of Efficient PBDB-T: PZT-Based All-Polymer Solar Cell: Role of Band Alignment, *Polym.* **15**(4), 869 (2023). https://doi.org/10.3390/polym15040869.
5. N. I. M. Ibrahim, A. M. Elharbi, and A. Albadri, Study the Effect of Thickness on the Performance of PM6:Y6 Organic Solar Using SCAPS Simulation, *Adv. Mater. Phys. Chem.* **14**(14), 55 (2024). https://doi.org/10.4236/ampc.2024.144005.
6. S. A. Obaid, F. A. Senaed, and B. Y. Kadem, Impact of i-Layer Thickness on Band Alignments of a-Si:H Solar Cells: A Simulation Study Using SCAPS Software, *Iraqi J. Appl. Phys.* **22**(1), 62 (2026).
7. M. Li, P. Huang, and H. Zhong, Current Understanding of Band-Edge Properties of Halide Perovskites: Urbach Tail, Rashba Splitting, and Exciton Binding Energy, *J. Phys. Chem. Lett.* **14**(6), 1592 (2023). https://doi.org/10.1021/acs.jpclett.2c03525.
8. B. Bratina and E. Pavlica, Characterization of Charge Carrier Transport in Thin Organic Semiconductor Layers by Time-of-Flight Photocurrent Measurements, *Org. Electron.* **64**, 117 (2019). https://doi.org/10.1016/j.orgel.2018.09.049.
9. W. Miao, Y. Liu, Y. Wu, J. Liang, J. Xiong, T. Hu, Y. He, L. Chen, J. Shan, X. Wang, and R. Yang, Energy Disorder Suppression, Charge Transport Channel Establishment by Integrating Four-Arm Donor Molecule for High-Performance Organic Solar Cells, *Adv. Funct. Mater.* **35**(32), 2501143 (2025). https://doi.org/10.1002/adfm.202501143.
10. N. Tokmoldin, S. M. Hosseini, M. Raoufi, L. Q. Phuong, O. J. Sandberg, H. Guan, Y. Zou, D. Neher, and S. Shoaee, Extraordinarily long diffusion length in PM6:Y6 organic solar cells, *J. Mater. Chem. A*. **8**(16), 7854 (2020). https://doi.org/10.1039/D0TA03016C.
11. F. Jannat, S. Ahmed, and M. A. Alim, Performance analysis of cesium formamidinium lead mixed halide based perovskite solar cell with MoO_x as hole transport material via SCAPS-1D, *Optik.* **228**, 166202 (2021). https://doi.org/10.1016/j.ijleo.2020.166202.
12. S. Chauhan and R. Singh, Unlocking the efficiency potential of tin-based perovskite solar cell, *Pramana.* **98**(1), 28 (2024). https://doi.org/10.1007/s12043-023-02714-x.
13. B. Y. Kadem and R. F. Alfahed, Non-Fullerene OSC: The Effects of Active and Electron Transport Layers' Thickness Towards 19.5% efficiency, *JREEN* **28**(1), 39 (2025). https://doi.org/10.54966/jreen.v28i1.1275.
14. B. Y. Kadem, A. K. Hassan, and W. M. Cranton, Efficient P3HT:PCBM bulk heterojunction organic solar cells; effect of post deposition thermal treatment, *J. Mater. Sci. Mater. Electron.* **27**, 7038 (2016). https://doi.org/10.1007/s10854-016-4661-8.
15. C. Chen, G. Wen, Z. Xiao, J. Peng, R. Hu, Z. Chen, C. Zhang, and W. Zhang, Charge Photogeneration and Recombination Dynamics in PTQ10:Y6 Solar Cells, *Photonics* **9**, 892 (2022). https://doi.org/10.3390/photonics9120892.
16. M. E. A. Boudia, Q. Wang, and C. Zhao, Optimization of the Active Layer Thickness for Inverted Ternary Organic Solar Cells Achieves 20% Efficiency with Simulation, *Sustainability* **16**(14), 6159 (2024). https://doi.org/10.3390/su16146159.
17. T. Kirchartz, T. Agostinelli, M. Campoy-Quiles, W. Gong, and J. Nelson, Understanding the Thickness-Dependent Performance of Organic Bulk Heterojunction Solar Cells: The Influence of Mobility, Lifetime, and Space Charge, *J. Phys. Chem. Lett.* **3**(23), 3470 (2012). https://doi.org/10.1021/jz301639y.
18. D. He, L. Xie, Y. Bai, H. Zhang, L. Liu, J. Kong, Y. Chai, X. Li, M. Wang, Y. Zhang, and J. Zhang, Achieving High Fill Factor via Increasing Interfacial Disorder to Inhibit Bimolecular Recombination for Efficient Organic Solar Cells, Angew. Chem. Int. Ed., e202505722 (2025). https://doi.org/10.1002/anie.202505722.
19. V. Magnin and K. N'konou, Numerical Study of Charge Transport Layers in Inverted Ternary Organic Photovoltaic Cells, *EPJ Photovoltaics* **15**, 29 (2024). https://doi.org/10.1051/epjpv/2024024.

20. G. Kumar, E. Lakhwani, W. Elmalem, W. T. S. Huck, A. Rao, N. C. Greenham, and R. H. Friend, Interface Limited Charge Extraction and Recombination in Organic Photovoltaics, *Energy Environ. Sci.* **7**(7), 2227 (2014). https://doi.org/10.1039/C4EE00665H.
21. N. Gasparini, A. Salleo, I. McCulloch, and D. Baran, The Role of the Third Component in Ternary Organic Solar Cells, *Nat. Rev. Mater.* **4**(4), 229242 (2019). https://doi.org/10.1038/s41578-019-0093-4.
22. K. Wang, C. Sun, C. Zhang, H. Bai, S. Sang, Y. Li, Z. Chen, J. Hu, X. Li, L. Meng, and Y. Li, Fine-Tuning of Film Morphology Through Addition of a Third Component Enables Organic Solar Cells with Efficiency Over 18%, *Mater. Chem. Front.* **8**, 1 (2024). https://doi.org/10.1039/D4QM00231H.
23. G. Ding, S. T. Han, C.C. Kuo, V.A. Roy, and Y. Zhou, Porphyrin-Based Metal–Organic Frameworks for Neuromorphic Electronics, *Small Structures*, **4**(2), 2200150 (2023). https://doi.org/10.1002/sstr.202200150.
24. H. Lu *et al.*, Simultaneously Enhancing Exciton/Charge Transport in Organic Solar Cells by an Organoboron Additive, *Adv. Mater.* **34**(42), 2205926 (2022). https://doi.org/10.1002/adma.202205926.
25. A. Mahmoudloo, Investigation of Charge Carrier Transport and Recombination in Organic Semiconductors with Charge Extraction by Linearly Increasing Voltage (CELIV) Technique, *J. Appl. Res. Ind. Eng.* **10**(4), 575-583 (2023). https://doi.org/10.22105/jarie.2022.344217.1474.
26. J. Važgėla, K. Genevičius, and G. Juška, A Positivity-Preserving, Implicit Defect-Correction Multigrid Method for Turbulent Combustion, *Chem. Phys.* **478**, 126 (2016). https://doi.org/10.1016/j.chemphys.2016.04.005.
27. D. Meng, J. Xue, Y. Zhao, E. Zhang, R. Zheng, and Y. Yang, Configurable Organic Charge Carriers toward Stable Perovskite Photovoltaics, *Chem. Rev.*, **122**(18) (2022), 14954. https://doi.org/10.1021/acs.chemrev.2c00166.
28. X. Du, X. Li, Q. Chen, H. Lin, and S. Tao, High performance organic solar cells based on ZnO: POT2T as an effective cathode interfacial layer, in *J. Phys.: Conf. Ser.* **1549**, 042015 (2020). https://doi.org/10.1088/1742-6596/1549/4/042015.
29. H. Zerfaoui, D. Dib, and B. Y. Kadem, The Simulated Effects of Different Light Intensities on the SiC-Based Solar Cells, *Silicon* **11**(4), 1917 (2019). https://doi.org/10.1007/s12633-018-0011-1.
30. Y. Kong, H. Chen, and L. Zuo, Understanding the Nonradiative Charge Recombination in Organic Photovoltaics: From Molecule to Device, *Adva. Funct. Mater.* **35**(3), 2413864 (2025). https://doi.org/10.1002/adfm.202413864.

إشكالية السُمك باستخدام أسلوب المحاكاة: تحليل أداء الخلايا الشمسية العضوية المعتمدة علىPM6:Y6

ضحى إسماعيل خليل[1] ودانيا ظافر حميد[2] وهناء محمد نجم[3] وبراق يحيى كاظم[2]

[1] كلية علوم الطاقة والبيئة، جامعة الكرخ للعلوم، بغداد، العراق

[2] كلية العلوم، جامعة الكرخ للعلوم، بغداد، العراق

[3] كلية العلوم، جامعة بغداد، بغداد، العراق

الخلاصة

دُرسَ تأثير سُمك الطبقة النشطة على أداء الخلايا الشمسية العضوية PM6:Y6 باستخدام عدة تقنيات توصيف، مثل منحنى كثافة التيار مقابل الجهد (J-V)، ومنحنى السعة مقابل الجهد (C-V)، ومنحنى الشحنة مقابل الجهد (Q-V)، واستخلاص الشحنة بزيادة الجهد خطيًا (CELIV)، والقياسات المعتمدة على شدة الإضاءة الشمسية. أظهرت النتائج أن زيادة السُمك تزيد من امتصاص الضوء، وبالتالي كثافة تيار الدائرة القصيرة (JSC)، ولكن السُمك المفرط يُسبب قيودًا على النقل وزيادة في إعادة التركيب، مما يؤدي إلى انخفاض عامل الملء (FF). من ناحية أخرى، ظل جهد الدائرة المفتوحة (VOC) ضعيف الاعتماد على تغير السُمك. ونتيجة لذلك، زادت كفاءة تحويل الطاقة (PCE) في البداية ثم انخفضت بعد تجاوز السُمك الأمثل. أشارت نتائج C-V و Q-V إلى انخفاض كفاءة استخلاص الشحنة وزيادة المقاومة التسلسلية في الأغشية السميكة. أظهرت تحليلات إعادة التركيب والحركية معدلات فقد أعلى وحركية فعالة أقل مع زيادة السُمك، بما يتوافق مع مسارات نقل أطول. أكدت تقنية CELIV نقلًا أكثر تشتتًا ومحدودًا بالفخاخ في الطبقات السميكة. أظهرت قياسات JSC المعتمدة على شدة الضوء اعتمادًا شبه خطي ($\alpha \approx 1$)، وأظهرت قياسات Suns-VOC جهدًا غير حساس للسمك تحكمه بشكل رئيسي حركية إعادة التركيب.

الكلمات المفتاحية: مزيج بوليمر/مستقبل عضوي، الخلايا الشمسية العضوية، إعادة الاتحاد، الاعتماد على السُمك، الخلايا الشمسية المُحاكاة